Semicond. Sci. Technol. 9 (1994) 263–271. Printed in the UK

Electronic structure of Si δ-doped GaAs in an electric field

F Domínguez-Adame, B Méndez and E Maciá

Departamento de Física de Materiales, Facultad de Físicas, Universidad Complutense, E-28040 Madrid, Spain

Received 9 November 1993, accepted for publication 5 January 1994

Abstract. The electron dynamics and the density of states of both single and periodic Si δ-doped GaAs subject to an applied electric field are studied theoretically. The space charge potential due to δ-doping is obtained by means of the semiclassical Thomas–Fermi model. Analysing the change in the density of states introduced by the δ-doping plus the electric field, we observe a set of sharp peaks, corresponding to field-induced localized states, and subsidiary peaks associated with more extended states. Furthermore, we use the inverse participation ratio to evaluate the spatial extent of electron wavefunctions. The number of sharp peaks equals the number of δ-doped layers. In the case of periodically δ-doped samples, the sharp peaks are equally spaced and give rise to Stark ladder resonances.

1. Introduction

Epitaxial growth techniques, such as molecular beam epitaxy (MBE), are currently used to prepare δ-doped semiconductor structures, in which a thin slab of impurity atoms is localized within few monolayers of the crystal. Impurity atoms usually supply electrons and give rise to strong confinement by space charge potential, as was found in the case of Si δ-doped GaAs [1], hence forming a quasi-two-dimensional electron gas. Single and multiple δ-doped systems are being intensively investigated from both experimental [2–5] and theoretical [6–9] points of view because of their numerous potential applications in semiconductor devices (see [10] for some examples of how δ-doping might offer practical advantages). Furthermore, these structures are a source of basic research on related problems, such as electron localization in two-dimensional systems due to the random distribution of impurities in the doping layer.

Overlap of the electron wavefunctions of adjacent layers in periodically δ-doped structures causes the formation of subbands, as observed experimentally by Shubnikov–de Haas techniques [4] and optical measurements [11] in Si δ-doped GaAs. Since the space charge potential is strongly dependent on the impurity concentration, the dispersion relation along the growth direction will depend on both impurity concentration and doping period. Some information about the Fermi surface and energy gaps between minibands can be inferred from photoluminescence (PL) measurements, as demonstrated theoretically by Henriques *et al* [9]. From this study one might expect that PL measurements at low temperatures could provide valuable information regarding the space charge potential and the interaction of electrons with the doping layer. Nevertheless, it is to be expected that the presence of an applied electric field will modify the subband structure of multiple δ-doped GaAs. Therefore, the theoretical analysis of the resulting electronic structure of the superlattice subject to an electric field becomes a valuable task.

After many years of controversy, it is now recognized that an electric field applied across a periodic structure leads to the occurrence of the so-called Stark ladder resonances (see [12] for a brief historical survey of the evolution of this controversy). These ladders are not infinitely sharp levels—as was proposed originally—but they are resonant levels whose lifetimes are finite. The Stark ladder structure is characterized by a series of resonances separated by an energy eFa, where e is the absolute value of the electron charge, F stands for the applied electric field, and a denotes the spatial period of the periodic structure. In actual solids, a is of order of the lattice parameter, so that one would require very high electric fields to clearly observe a well-separated ladder structure, with the level spacing larger than the level width. Technological progress on superlattices has made it possible to fabricate artificial structures with very long period and extremely high quality, hence making observation of the ladder structure easier. In fact, recent experiments seem to firmly establish the existence of a ladder structure in quantum well superlattices [13–16]. From a theoretical point of view, most works have considered so far either an array of δ-function potentials [12, 17] or periodic Kronig–Penney potentials with an applied electric field [18–20]. The latter potential is useful for describing quantum well structures within the effective-mass approximation. It is

0268-1242/94/030263+09$19.50

reasonable to think that an electric field along the growth direction in multiple δ-doped semiconductors may lead to phenomena similar to those observed in quantum well superlattices. As far as we know, however, the possible occurrence of Stark ladders in such structures has not been investigated.

In the present work we study theoretically the electron dynamics and the density of states in both single and periodically Si δ-doped GaAs under homogeneous applied electric fields, as well as the influence of the impurity concentration on electronic properties. The space charge potential is found by solving the Thomas–Fermi equation. Since no analytical expressions for the space charge potential due to the doping layer exist†, we have developed a numerical technique to solve the corresponding Schrödinger equation and to find the change in the density of states (DOS) introduced by the structure. We shall show that Stark ladder resonances are clearly observed in the DOS, hence suggesting that this spectrum should also be observable experimentally in periodically δ-doped structures, as was the case in quantum well superlattices.

The paper is organized as follows. In section 2 we briefly discuss our model, in which the space charge potential due to Si δ-doping in GaAs is found by means of the semiclassical Thomas–Fermi formulation. Therefore the many-body problem reduces to studying the dynamics of a single electron within the effective-mass approach. Section 3 is devoted to describing the numerical method used to obtain (i) bound states in zero-field single δ-doped layers, (ii) subband structure in periodically δ-doped structures and (iii) the change in the density of states and electron localization due to the presence of the structure plus the electric field. Results and discussions are collected in section 4; for the sake of clarity, results obtained in single and multiple structures (with and without applied electric field) are discussed separately. Finally, section 5 summarizes our results.

2. The model

The system we study in this work is a semiconductor structure made of Si δ-doped GaAs. The unit cell is a slab of GaAs of thickness a, with a Si δ-doping layer embedded in its centre. We assume that there exists a uniform p-type background doping with N_A acceptors per unit volume, and that the doping layer consists of a continuous positive slab of thickness d with N_D ionized donors per unit area. The whole structure consists of N unit cells sandwiched between two buffer layers of GaAs, each of thickness b. The total thickness of the system then is $L = Na + 2b$.

We calculate the space charge potential $V(x)$ (x denotes the spatial coordinate perpendicular to the layers) in the unit cell by means of the Thomas–Fermi (TF) semiclassical model. The many-body exchange and correlation effects are known to be small in the present system and they will be neglected completely [3]. The TF formulation has been demonstrated to be equivalent to the self-consistent formulation over a wide range of doping concentrations [6], and it has been considered previously in regard to zero-field periodically δ-doped structures by Egues *et al* [4]. The nonlinear TF differential equation in that case is

$$\frac{d^2V(x)}{dx^2} = -\frac{8}{3\pi}[\epsilon_F - V(x)]^{3/2} + \frac{8\pi}{d}N_D\theta\left(x+\frac{d}{2}\right)\theta\left(x-\frac{d}{2}\right) - 8\pi N_A\theta\left(x+\frac{a}{2}\right)\theta\left(x-\frac{a}{2}\right) \quad (1)$$

where ϵ_F denotes the Fermi energy. Distances have been scaled by the effective Bohr radius of the impurity, a^*, and energies by the effective Rydberg, Ry*. In the case of Si δ-doped GaAs these parameters are $a^* = 100$ Å and Ry* = 5.8 meV. Equation (1) is solved numerically under superlattice boundary conditions [4]

$$\left(\frac{dV(x)}{dx}\right)_0 = \left(\frac{dV(x)}{dx}\right)_{a/2} = 0. \quad (2)$$

These boundary conditions allow us to calculate $V(x)$ in the right half unit cell $[0, a/2]$. Since we are assuming a symmetrical doping profile, the potential in the left half is found using $V(-x) = V(x)$.

We assume the validity of the effective-mass approximation, and we take an isotropic and parabolic conduction band in the growth direction. This approximation usually works fine in GaAs, except at very high electric fields, when the Γ–X mixing induced by the field occurs [21]. Thus, once the potential $V(x)$ is found from (1), the electron dynamics in the unit cell along x in the presence of a homogeneous applied electric field, perpendicular to the doping layers, is obtained from the following one-dimensional Schrödinger equation:

$$-\frac{d^2\psi(x)}{dx^2} + [eFx + V(x)]\psi(x) = E\psi(x). \quad (3)$$

To solve the Schrödinger equation (3) we must set appropriate boundary conditions at the edges of the system. This is not a trivial question, as pointed out by Banavar and Coon [18], in order to obtain a correct account of Stark ladder resonances. For instance, infinite barriers at the edges of the system may convert resonance states into zero-width bound states. Reasonable boundary conditions consist of letting the potential level off at the value it has at the edges of the crystal [18]. The potential used in our calculations is sketched in figure 1; the origin of the spatial coordinate is set at the left edge of the system while energies are measured from the potential value at that edge. Accordingly, the electron behaves as a free particle for $x < 0$ and $x > L$. In GaAlAs-based quantum well

† Ioriatti [6] finds an analytical result in the case of a single layer when the doping profile is assumed to be a δ-function profile in the Poisson equation.

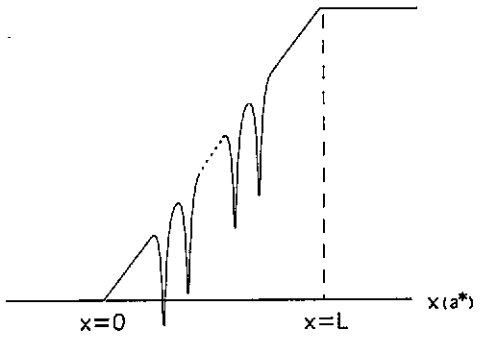

Figure 1. Potential profile of a superlattice consisting of N δ-doped layers of width a under an applied external field, used in our calculations.

structures, Ritze *et al* [20] have found that the spectra embody the occurrence of Stark ladder structure in the energy range $0 < E < eFL$, whereas the the range $E > eFL$ is dominated by two kinds of structure, one similar to Franz–Keldysh oscillations and another resembling the Stark ladder behaviour. In our preliminary studies we found that an analogous statement holds for periodically δ-doped GaAs, namely that Stark levels are more clearly observed below the top of the ramp, so we will be concerned with those states hereafter.

3. Numerical analysis

Consider an electron of energy E impinging from the left on the structure shown in figure 1. Since we are assuming that $0 < E < eFL$ the electron will be reflected with probability 1. Therefore, the reflection amplitude can be expressed as

$$r = \mathrm{e}^{2\mathrm{i}\Phi(E)} \tag{4}$$

where the phase shift $\Phi(E)$ is real. The definition of the density of states (DOS) for systems displaying continuous energy spectra presents some problems [20], while the change in the DOS introduced by the considered structure is a well defined parameter [22]. Levinson's theorem relates this phase shift and the change in the DOS, $\Delta\rho(E)$, through the equation [23]

$$\Delta\rho(E) = \frac{1}{2\pi}\frac{\mathrm{d}\Phi(E)}{\mathrm{d}E}. \tag{5}$$

The reflection amplitude is found by solving the Schrödinger equation (3). Since there is no analytical expression for the potential $V(x)$, computation of r must resort to numerical procedures. To this end, we divide the interval into a grid of points $\{x_k = kh\}$, where $h = a/l$ is the integration step and l is the number of grid points in each unit cell. The discretized form of the Schrödinger equation (3) may be cast in the matrix form

$$\begin{pmatrix} \psi(x_{k+1}) \\ \psi(x_k) \end{pmatrix} = \begin{pmatrix} \alpha_k & -1 \\ 1 & 0 \end{pmatrix} \begin{pmatrix} \psi(x_k) \\ \psi(x_{k-1}) \end{pmatrix} \equiv P_k \begin{pmatrix} \psi(x_k) \\ \psi(x_{k-1}) \end{pmatrix} \tag{6}$$

where we have defined $\alpha_k \equiv 2 + h^2[V(x_k) + eFx_k - E]$ for brevity. This form is suitable for a transfer-matrix approach to solving the scattering problem [24]. In fact, iterating this equation gives

$$\begin{pmatrix} \psi(x_{N_s+1}) \\ \psi(x_{N_s}) \end{pmatrix} = P_{N_s} \ldots P_0 \begin{pmatrix} \psi(x_0) \\ \psi(x_{-1}) \end{pmatrix} \equiv T(N_s) \begin{pmatrix} \psi(x_0) \\ \psi(x_{-1}) \end{pmatrix}. \tag{7}$$

$T(N_s)$ is the transfer matrix of the whole system and N_s is the number of grid points in the whole structure. $T(N_s)$ is real and relates the wavefunction at both edges of the structure. The solution of the wave equation in the field-free region is given by

$$\psi(x_k) = \begin{cases} \mathrm{e}^{\mathrm{i}q_l k} + r\mathrm{e}^{-\mathrm{i}q_l k} & k \leqslant 0 \\ \mathrm{e}^{-q_r k} & k \geqslant N_s \end{cases} \tag{8}$$

where $q_l \equiv h\sqrt{E}$ and $q_r \equiv h\sqrt{eFL - E}$ for small h. Both parameters are real for the energy range considered. Using (7) and (8), we have

$$r = -\frac{T_{11}(N_s) - T_{21}(N_s)\mathrm{e}^{-q_r} + [T_{12}(N_s) - T_{22}(N_s)\mathrm{e}^{-q_r}]\mathrm{e}^{-\mathrm{i}q_l}}{T_{11}(N_s) - T_{21}(N_s)\mathrm{e}^{-q_r} + [T_{12}(N_s) - T_{22}(N_s)\mathrm{e}^{-q_r}]\mathrm{e}^{\mathrm{i}q_l}}. \tag{9}$$

Notice that this numerical procedure preserves the unimodularity of the reflection amplitude. This amplitude may be recursively computed from the matrix elements of $T(N_s)$. Taking into account that $T(k) = P_k T(k-1)$ and $T(0) = P_0$, we find the following recurrence relations involving only real parameters:

$$\begin{aligned} T_{11}(k) &= \alpha_k T_{11}(k-1) - T_{11}(k-2) \\ T_{12}(k) &= \alpha_k T_{12}(k-1) - T_{12}(k-2) \\ T_{21}(k) &= T_{11}(k-1) \\ T_{22}(k) &= T_{12}(k-1) \qquad k = 1, 2 \ldots N_s. \end{aligned} \tag{10}$$

These equations must be supplemented with the initial conditions $T_{ij}(-1) = \delta_{ij}$, $T_{11}(0) = \alpha_0$, $T_{12}(0) = -1$, $T_{21}(0) = 1$ and $T_{22}(0) = 0$.

It is worth mentioning that this transfer-matrix technique can also be applied to obtain the bandgaps and the dispersion relation inside subbands in general periodic potentials [24], with particular application to zero-field periodically δ-doped structures. Since the Bloch theorem must be satisfied, the dispersion relation is found to be (see [24] for details)

$$\cos(\kappa_\parallel a) = \tfrac{1}{2}\,\mathrm{Tr}[T(l)] \tag{11}$$

where $\kappa_\parallel$ is the crystal momentum along the growth direction. The required symmetry of the dispersion relation $E(-\kappa_\parallel) = E(\kappa_\parallel)$ is conserved. Real values of the crystal momentum give the dispersion relation inside allowed subbands.

This numerical technique may be easily modified to obtain bound states of a single δ-doped well in a straightforward fashion. Since outside the well the wavefunction of bound states is of the form $\psi(x_k) \sim \exp\left(-h|k|\sqrt{-E}\right)$, after some algebra one obtains that bound levels are the roots of the equation

$$T_{11}(l)e^{h\sqrt{-E}} - T_{22}(l)e^{-h\sqrt{-E}} + T_{12}(l) - T_{21}(l) = 0 \quad (12)$$

where $T_{ij}(l)$ are to be computed recursively as before. Standard search methods are then used to obtain bound state energies. We should mention that in (11) and (12) integration is performed over a single layer, and consequently computations are fairly fast. Unfortunately, this is not the case in multiple δ-doped GaAs with an external electric field because the index k in (10) runs over the whole structure.

4. Results and discussions

We have studied the electronic structure of single and periodically Si δ-doped GaAs with doping period a = 500 Å, donor concentration N_D ranging from 0.5 up to 5×10^{12} cm^{-2} uniformly distributed over d = 50 Å, and a p-type background doping of $N_A = 1\times10^{15}$ cm^{-3}. These parameters, taking $N_D = 3 \times 10^{12}$ cm^{-2}, correspond to the MBE samples grown by Egues *et al* [4]. The number of δ-doped layers N varies between 1 and 10, sandwiched between two b = 1000 Å buffer layers of GaAs. The TF potential was found by solving (1) and (2) using standard methods. To solve the corresponding Schrödinger equation (3), each unit cell was divided into l = 600 grid points, which are enough to obtain very accurate results. The doping period a = 500 Å is intermediate between two limiting cases discussed by Degani [7]. This author found by self-consistent calculations that for a long period ($a \sim$ 1000 Å) the system behaves as single doping, whereas for a short period ($a \sim$ 200 Å) a superlattice is formed due to strong coupling between adjacent wells. Therefore, our study acquires the additional importance of assessing the effect of moderate coupling in the electronic structure. We carry out a systematic study of bound states of single δ-doped layers, subbands in periodically δ-doped layers and reflection amplitude behaviour (and the change in the DOS) in biased structures, computed according to the methods described in the preceding section.

4.1. Single Si δ-doped GaAs with $F = 0$

We first give results for single Si δ-doped GaAs without applied electric field. Figure 2 shows the calculated TF potential for different donor concentrations, choosing the origin of the spatial coordinate at the middle of the unit cell. The TF potential is deeper for larger doping, whereas the top of the potential remains almost unchanged. Notice that energies are referred to the Fermi level and not to the top of the potential in this figure; this allows a direct comparison with previous results of

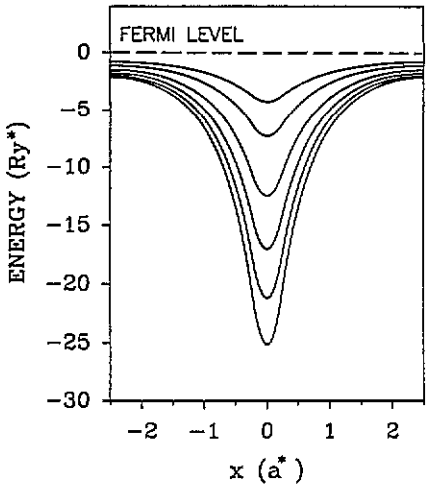

Figure 2. TF potential due to a single δ-doped layer obtained by solving the corresponding TF equation. From top to bottom N_D = 0.5, 1, 2, 3, 4 and 5 × 10^{12} cm^{-2}, distributed over 50 Å.

Egues *et al* [4] and other authors, who take ϵ_F as the zero of energy. When the electric field is applied, however, we measure energies from the value of the potential at the left edge of the system.

As we mentioned earlier, the period a = 500 Å yields weak coupling between adjacent wells. Therefore, lower subbands will be only slightly broadened because electrons are tightly bound. Hence it would be instructive to find bound state levels of an isolated well in order to compare them with subband structure in multiple δ-doped systems. We have used (12) to compute energy levels as a function of donor concentration, as shown in figure 3. As expected, the number of bound states increases with donor concentration: at low doping only one bound state is supported, while at high doping (larger than about 2 × 10^{12} cm^{-2}) three bound states appear.

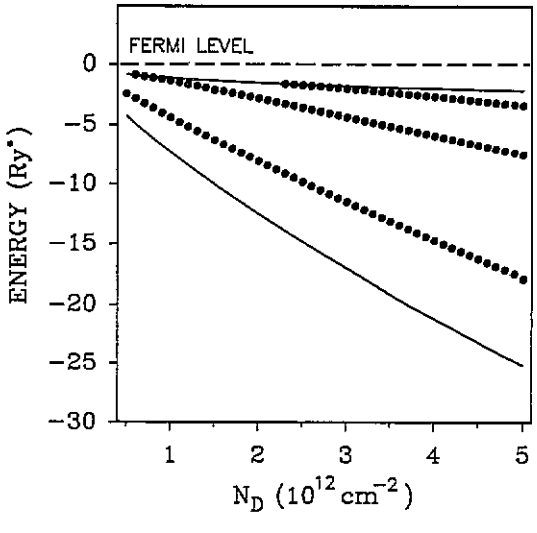

Figure 3. Bound state energies of a single TF potential as a function of the donor concentration (dotted curves). Top and bottom values of the potential are also indicated (full curves).

4.2. Single Si δ-doped GaAs with $F \neq 0$

In the method of phase-shift analysis, resonances are characterized by a rapid increase of π in the phase $\Phi(E)$. Hence the change in the DOS exhibits peaks accordingly. We observe these peaks when an external electric field is applied, as shown in figure 4 for a single δ-doped layer of $N_D = 3 \times 10^{12}$ cm^{-2} with $F = 20$ kV cm^{-1} (DOS will be expressed in arbitrary units because we are mainly interested in the position and width of these peaks). In figure 4(a) two resonances are clearly seen in the change in the DOS, centred at about 36.3 Ry* and 41.3 Ry*. Resonances occur whenever the energy of the incident electron matches one of the quasi-levels of the well (see also figure 4(b)). The first one is below the barrier (i.e. below the local maximum of the potential, placed at about $x = 11a^*$ with barrier height about 40.0 Ry*), whereas the second one is above. As a consequence, the resonance below the barrier is much narrower and higher because its lifetime is much longer. Figure 5 shows the Lorentzian shape of the lowest resonance; this shape is expected from quantum-mechanical scattering theory. The narrow resonance is associated with a well-localized electronic wavefunction, whereas the wider resonance corresponds to an extended wavefunction, as seen in figure 6.

In our computations we found that both resonance width (FWHM), Γ, and peak position, E_p, are strongly dependent on the applied electric field. With increasing field the peaks shift and become broader and lower. As observed from figure 7, where Γ is plotted versus F^{-1} for the two resonances appearing in figure 4(a), this dependence can be expressed approximately as

$$\Gamma(F) = Ae^{-B/F} \tag{13}$$

where the parameters A and B depend on the donor concentration and the particular resonance examined. For instance, B is largest for the lowest resonance (see

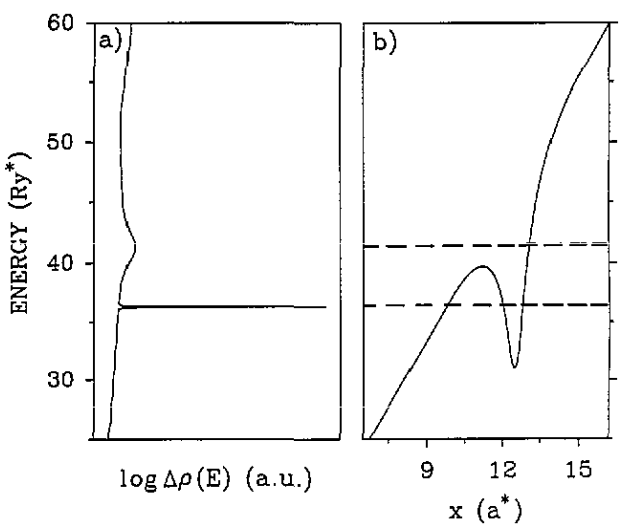

Figure 4. (a) Change in the DOS versus energy for a single δ-doped layer with a donor concentration of $N_D = 3 \times 10^{12}$ cm^{-2} subject to an applied electric field $F = 20$ kV cm^{-1}, and (b) a detailed view of the potential versus position. Broken lines indicate the energy of the resonances.

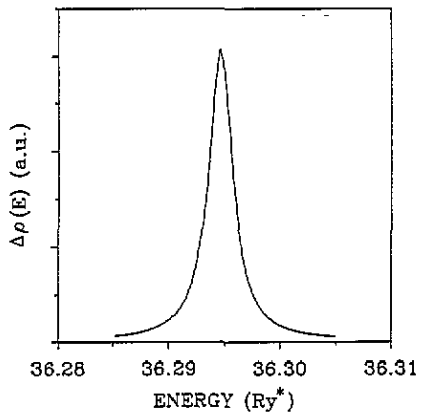

Figure 5. Linear-scale plot of the change in the DOS versus energy corresponding to the narrow resonance of figure 4, showing its Lorentzian shape.

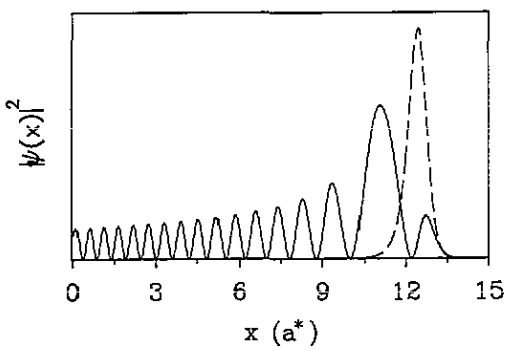

Figure 6. Squared electron wavefunction corresponding to the narrow (broken curve) and broad (full curve) resonances of figure 4.

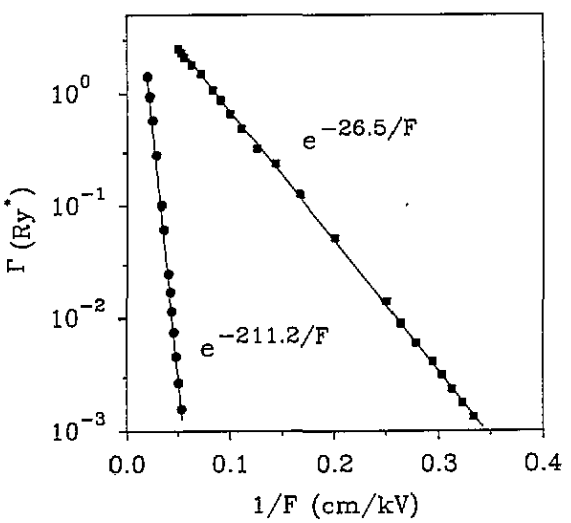

Figure 7. Resonance width (FWHM) on a log scale as a function of the electric field for the lower (circles) and higher (squares) resonances of figure 4.

figure 7). On the other hand, the position of resonances as a function of the applied electric field is of the form

$$E_p = \tfrac{5}{2}eaF + E_p^0 \tag{14}$$

as shown in figure 8 for $N_D = 3 \times 10^{12}$ cm^{-2}. The factor $\frac{5}{2}$ comes from the fact that the Si layer is placed at $x = \frac{5}{2}a$. The parameter E_p^0 gives the position of

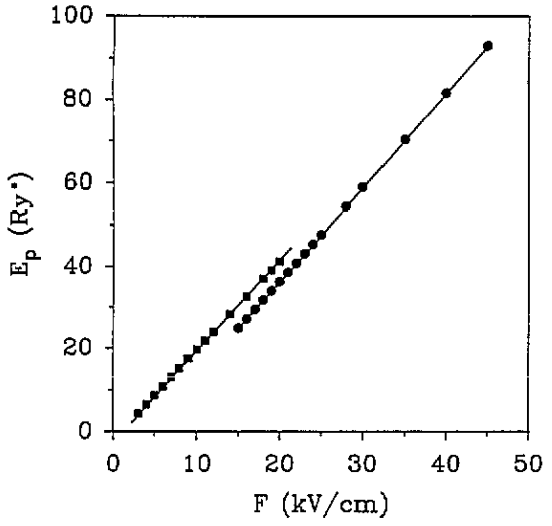

Figure 8. Resonance energy as a function of the electric field of the lower (circles) and higher (squares) resonances of figure 4. Extrapolation to $F = 0$ gives the energy of the corresponding (zero-field) bound state measured from the top of the potential.

resonances in the limit $F \to 0$, that is, when resonances turn into truly bound states. In the case of $N_D = 3 \times 10^{12}$ cm^{-2} depicted in figure 8 we find that E_p^0 is -2.21 Ry* and -9.10 Ry* for the upper and lower resonances respectively. These values are in good agreement with the energy of the bound states obtained from (12) and shown in figure 3, measured from the top of the potential well.

4.3. Periodically Si δ-doped GaAs with $F = 0$

In this section we deal with subband structure of periodically Si δ-doped GaAs, obtained by means of (11). Figure 9(*a*) shows a plot of the subbands for a donor concentration $N_D = 3 \times 10^{12}$ cm^{-2}. Note that lower subbands are slightly broadened (their widths are only 1×10^{-4} Ry* and 6×10^{-2} Ry*) and become

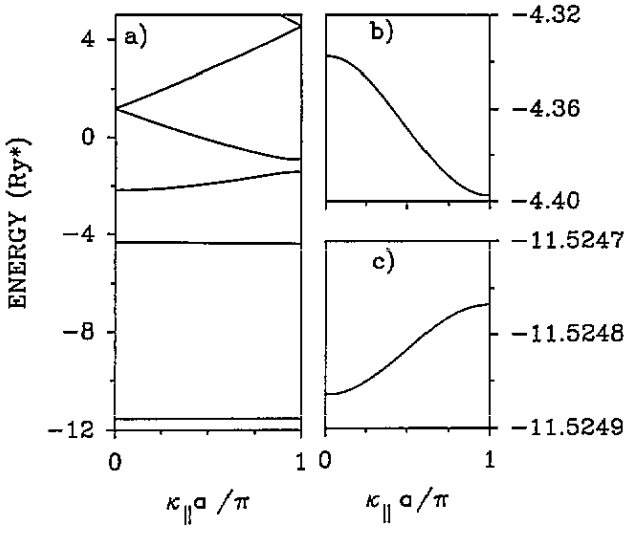

Figure 9. (*a*) Subband structure for periodically Si δ-doped GaAs with a donor concentration $N_D = 3 \times 10^{12}$ cm^{-2}. An enlargement of the two lower subbands is shown in (*b*) and (*c*).

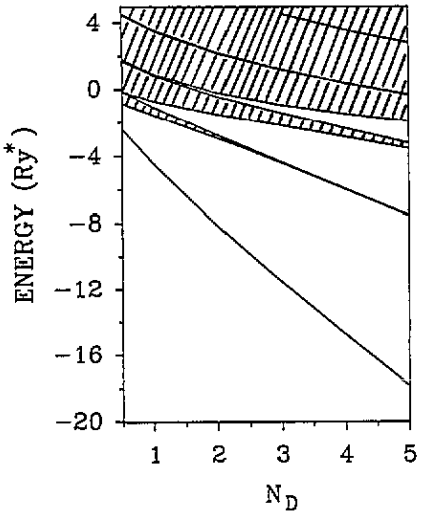

Figure 10. Allowed subbands (hatched regions) and gaps for periodically Si δ-doped GaAs as a function of the donor concentration.

almost non-dispersive, suggesting that these δ-doped layers are only weakly coupled. An enlargement of the two lower subbands is shown in figures 9(*b*) and (*c*). As we mentioned in section 4.1, the positions of these slightly dispersive subbands coincide with the energies of the lower bound states of single δ-doped layers. With increasing energy, gaps become narrower and subbands become broader.

Since the TF potential depends on N_D, it is to be expected that the subband structure is very sensitive to minor variations in the donor concentration. We actually found this result in our numerical study. Figure 10 shows allowed subbands and gaps as a function of donor concentration. We can observe that the lowest subband is almost non-dispersive over the whole range of donor concentration considered. However, the second subband becomes dispersive for concentrations less than $\sim 2 \times 10^{12}$ cm^{-2}.

4.4. Periodically Si δ-doped GaAs with $F \neq 0$

At zero field electronic states are delocalized and form bands. This picture remains valid even when a very low electric field is applied. However, on increasing the field, the quasi-levels of each well are shifted and quantum coherence is then reduced. The loss of quantum coherence causes field-induced Stark localization, implying the occurrence of sharp peaks in the change of the DOS. In this case $\Delta\rho(E)$ exhibits a set of N pronounced peaks separated equidistantly, as shown in figure 11 for two values of the applied electric field, $N = 10$ unit cells and $N_D = 1 \times 10^{12}$ cm^{-2}. Similar plots are observed for other values of the doping concentration. This pattern indicates that a well-defined Stark ladder structure is formed. In contrast to one-band, tight-binding Hamiltonians, the Schrödinger equation (3) includes all bands of the energy spectrum. As a consequence, more than one Stark ladder exists, each one evolving from a different zero-field subband, so that ladders may be labelled by the band index n. For

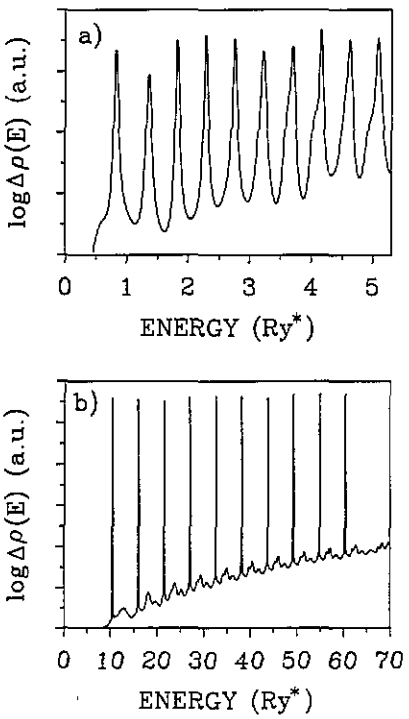

Figure 11. Change in the DOS versus electron energy for two different values of the applied electric field: (*a*) $F = 0.5$ kV cm^{-1} and (*b*) $F = 6.0$ kV cm^{-1}. The donor concentration is $N_D = 1 \times 10^{12}$ cm^{-2} in both cases.

instance, pronounced peaks of figure 11(*a*) correspond to $n = 2$ whereas those in figure 11(*b*) correspond to $n = 1$. It is also worth mentioning the occurrence of subsidiary peaks with increasing electric field; these peaks resemble small, broad peaks due to above-barrier states, previously discussed in the case of single δ-doping.

Resonance peaks arise from the interplay between two interactions, namely the coupling between different wells and the coupling with the applied electric field [20]. Since coupling between the δ-doping wells we are concerned with turns out to be rather weak, the second interaction dominates except at low field. This explains the absence of a perfect periodic pattern in $\Delta\rho(E)$ at low field, observed in figure 11(*a*), as due to the lack of spatial periodicity of the superlattice. Note, for instance, that the spacing between the two lower resonances is larger than the predicted value eFa, and also that shoulders appear in the higher resonances. Since Stark ladder states are rather localized, only states localized at the outermost wells (giving rise to lower and higher resonances) can feel the missing spatial periodicity. With increasing field, field-induced localization increases and the Stark state is confined into a single well due to a reduction of quantum coherence; then finite-size effects become less important. This leads to a well-defined Stark ladder structure, as seen in figure 11(*b*). In contrast, subsidiary peaks can feel finite-size effects, even at higher fields, because of their more extended character.

Figure 12 gives further evidence of the relation between the change in the DOS and localization of the electron wavefunction. Figure 12(*a*) shows a detailed

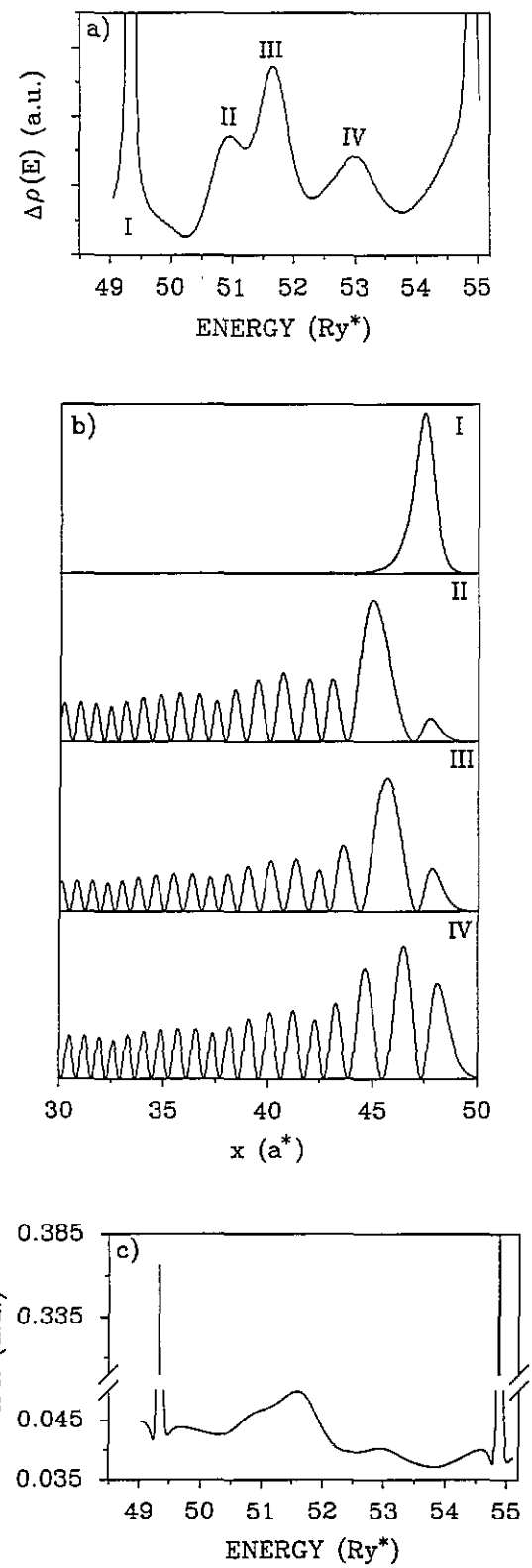

Figure 12. (*a*) Change in the DOS versus electron energy for $F = 6$ keV and $N_D = 1 \times 10^{12}$ cm^{-2}. (*b*) Squared electron wavefunction for energies corresponding to peaks marked by roman numerals in (*a*). (*c*) IPR versus energy.

view of the eighth Stark level (marked I) and subsidiary peaks (marked II, III and IV) corresponding to the same parameters as in figure 11(*b*). Electron wavefunctions at the energies of the different peaks are plotted in figure 12(*b*). It becomes clear that pronounced peaks correspond to rather localized states whereas subsidiary

peaks correspond to more extended states. In addtion, the degree of localization may be evaluated by means of the inverse participation ratio (IPR). The IPR gives an estimation of the volume occupied by the electron wavefunction: the smaller the IPR, the more extended the electron state. The IPR has been successfully used to study localization of Stark ladder states in tight-binding Hamiltonians by Leo and MacKinnon [25] and in GaAs–AlAs superlattices by Degani [19]. Figure 12(*c*) shows the IPR as a function of the electron energy. A comparison between figures 12(*a*) and (*c*) demonstrates that a pronounced peak in the change of the DOS, corresponding to Stark ladder states, yields a sharp peak in the IPR, implying that those states are strongly localized. In contrast, a subsidiary peak, corresponding to above-barrier states, yields a minor increase in the IPR, reflecting the fact that those states are rather delocalized. Therefore, the IPR confirms the results we discussed above.

With increasing field, the peaks corresponding to the same Stark ladder shift and become broader and lower. The position of the peaks, E_{nk} (n is the ladder index and $k = 0, 1 \ldots N-1$ runs over the peaks), depends linearly on the applied electric field, except for lower resonances at very low fields. Figure 13 shows results corresponding to the two Stark ladders shown in figure 11. The energy of Stark levels for not very low field is approximately given by

$$E_{nk} = (k + \tfrac{1}{2})eFa + E_n^0 \qquad (15)$$

where E_n^0 is roughly the energy of subband n. Extrapolation to $F \to 0$ of data appearing in figure 12 yields $E_2^0 = -0.17$ Ry* and $E_1^0 = -3.02$ Ry*, in good agreement with the centre of the second and the first subbands for $N_D = 1 \times 10^{12}$ cm^{-2}, respectively, measured from the top of the TF potential (see figure 10). Equation (15) is the generalization of (14) in the case of periodic δ-doping and it implies that the average level spacing is of the form eFa. In general, the shapes of

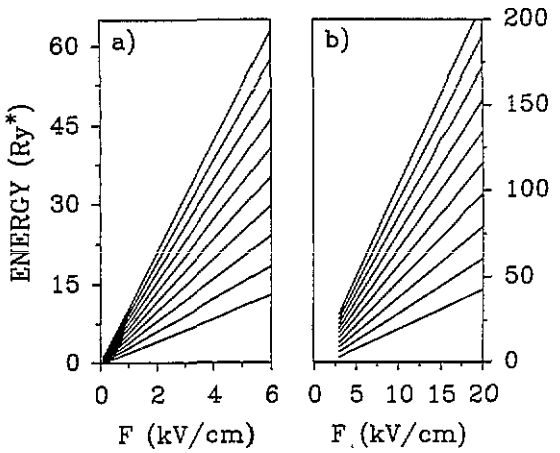

Figure 13. Energy of the Stark ladder levels as a function of the applied electric field. The donor concentration is $N_D = 1 \times 10^{12}$ cm^{-2}. Extrapolation of straight lines for $F \to 0$ gives the energy of the centre of zero-field subbands measured from the top of the TF potential: (*a*) second ladder, $E_2^0 = -0.17$ Ry*; (*b*) first ladder, $E_1^0 = -3.02$ Ry*. See text for further explanation.

Stark ladder resonances are fitted by Lorentzian curves, whose widths are given by (13). In our computations, all the widths turn out to be much smaller than the level spacing over the whole range of electric fields considered. This result suggests that Stark ladders may be observed in periodically δ-doped GaAs.

5. Concluding remarks

In the present work we have numerically investigated the electronic structure and the DOS of both single and multiple Si δ-doped GaAs. The space charge potential due to δ-doping is successfully evaluated by means of the semiclassical Thomas–Fermi method. We have also worked out a numerical method to compute bound states of single wells, subband structure in periodic superposition of δ-layers and the change in the DOS introduced by the structure subject to an applied electric field, parallel to the growth direction. In the absence of applied electric fields, lower subbands in periodic structures are only slightly broadened, because of the large doping period we consider (500 Å). Therefore the energies of these almost non-dispersive subbands coincide with the bound states of single δ-doped GaAs. Since electrons are then tightly bound, it is clear that tight-binding Hamiltonians could provide an easy way to obtain reliable information on the subband structure at low energies. When a single δ-doped layer is subject to an applied electric field, electronic states convert into resonances of finite lifetime, in a similar fashion to hydrogenic states in the presence of an external electric field (Stark effect). In the case of periodically δ-doped GaAs under an applied electric field, the occurrence of the well-known Stark ladders is observed in the change of the DOS. Each Stark ladder evolves from a different zero-field subband. Our results suggest that the interaction between different ladders is small, so that interband coupling should also be negligible. It is expected, however, that this coupling should increase on reducing the doping period. The Stark states are field-induced localized, indicating loss in the quantum coherence due to the misfit of local quasi-levels. Electronic states are pushed upwards and become broader as the electric field is increased, hence giving rise to the so-called above-barrier states. The IPR clearly shows that these states are less localized than Stark ladder states.

Some of the previous results have also been demonstrated to occur in quantum well superlattices. From an experimental point of view, however, significant differences between quantum well and δ-doped superlattices should appear. The model we have presented is not complete, in the sense that electron–phonon interactions and scattering by disorder have been omitted. We have found that the *intrinsic* broadening of levels, i.e. that predicted by scattering theory, is always larger than the level width. The physical relevance of this result is evident since one requires well-separated levels to be observable experimentally. Nevertheless, in

a real sample, broadening could be much larger than that predicted in our model. In the case of periodic δ-doping, broadening due to scattering by disorder might be more dramatic than in quantum well superlattices. The random distribution of donors in the δ-doped layers as well as fluctuations in their thickness may lead to a strong reduction of phase coherence. Finally, let us comment that, although our results indicate that Stark ladder resonances should be observable, experimental effort is needed to establish their existence. The availability of experimental data would greatly help in improving our model.

Acknowledgments

The authors are indebted to A Sánchez for a critical reading of the manuscript.

References

[1] Wood C E C, Metze G, Berry J and Eastman L 1980 *J. Appl. Phys.* **51** 383
[2] Cheng Wenchao, Zrenner A, Qiu-Yi Ye, Koch F, Grützmacher D and Balk P 1989 *Semicond. Sci. Technol.* **4** 16
[3] Koenraad P M, Blom F A P, Langerak C J G M, Leys M R, Perenboom J A A J, Singleton J, Spermon S J R M, van der Vleuten W C, Voncken A P J and Wolter J H 1990 *Semicond. Sci. Technol.* **5** 861
[4] Egues J C, Barbosa J C, Notari A C, Basmaji P, Ioriatti L, Ranz E and Portal J C 1991 *J. Appl. Phys.* **70** 3678
[5] Shibli S M, Scolfaro L M R, Leite J R, Mendonça C A C, Plentz F and Meneses E 1992 *Appl. Phys. Lett.* **60** 2895
[6] Ioriatti L 1990 *Phys. Rev.* B **41** 8340
[7] Degani M H 1991 *J. Appl. Phys.* **70** 4362
[8] Gold A, Ghazali A and Serre J 1992 *Semicond. Sci. Technol.* **7** 972
[9] Henriques A B and Gonçalves L C D 1993 *Semicond. Sci. Technol.* **8** 585
[10] Whall T E 1992 *Contemp. Phys.* **33** 369
[11] Maciel A C, Tatham M, Ryan J F, Worlock J M, Nahory R E, Harbinson J P and Florez L T 1990 *Surf. Sci.* **228** 251
[12] Chang M C and Niu Q 1993 *Phys. Rev.* B **48** 2215
[13] Bleuse J, Bastard G and Voison P 1988 *Phys. Rev. Lett.* **60** 220
[14] Agulló-Rueda F, Méndez E E and Hong J M 1989 *Phys. Rev.* B **40** 1357
[15] Digman M M and Sipe J E 1990 *Phys. Rev. Lett.* **64** 1797
[16] Saker M K 1991 *Phys. Rev.* B **43** 4945
[17] Cota E, José J V and Monsiváis G 1987 *Phys. Rev.* B **35** 8929
[18] Banavar J R and Coon D D 1978 *Phys. Rev.* B **17** 3744
[19] Degani M H 1991 *Appl. Phys. Lett.* **59** 57
[20] Ritze M, Horing N J M and Enderlein R 1993 *Phys. Rev.* B **47** 10437
[21] Hagon J P, Jaros M and Herbert D C 1989 *Phys. Rev.* B **40** 6420
[22] Trzeciakowski W and Gurioli M 1991 *Phys. Rev.* B **44** 3880
[23] Callaway J 1991 *Quantum Theory of the Solid State* (San Diego: Academic) p 400
[24] Méndez B, Domínguez-Adame F and Maciá E 1993 *J. Phys. A: Math. Gen.* **26** 171
[25] Leo J and MacKinnon A 1989 *J. Phys.: Condens. Matter* **1** 1449